# Synthesis and electrical properties of doped layered perovskites based on BaMInO$_4$ (M = Y, Gd)

Nataliia Tarasova [ab] * iD, Maxim Mashkovtsev [ab] iD, Maxim Domashenkov [ab],
Denis Khionin [ab], Roman Bastrikov [ab], Anzhelika Bedarkova [ab] iD

a: Institute of High Temperature Electrochemistry of the Ural Branch of the Russian Academy of Sciences, Ekaterinburg 620009, Russia

b: Institute of Hydrogen Energy, Ural Federal University, Ekaterinburg 620009, Russia

* Corresponding author: Natalia.Tarasova@ihte.ru
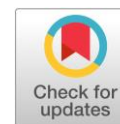
This paper belongs to a Regular Issue.

Abstract

Perovskite or perovskite-related structural materials are widely studied for their many functional properties. They can be used as components of electrochemical devices such as solid oxide fuel cells and electrolyzers. Layered perovskites can also be considered as promising materials for use in these devices. In this paper, the possibility of heterovalent (acceptor and donor) and isovalent doping of La and In sublattices of layered perovskites BaYLaInO$_4$ and BaGdLaInO$_4$ was made for the first time. The structure and electrical properties of these oxides were studied. Electrical conductivity values increase in the series BaYInO$_4$–BaLaInO$_4$–BaGdInO$_4$. However, the doping is an unsuitable strategy for improving the electrical properties of BaYInO$_4$ and BaGdInO$_4$ oxides. Further search for highly conductive materials with the layered perovskite structure can be aimed at materials with a different composition of the cation sublattice.

Key findings

● The success of the doping strategy for layered perovskites Ba(Sr)MInO$_4$ depends on the nature of the cations.

1. Introduction

The complex oxides with high temperature protonic conductivity are actively studied due to their potential applications in electrochemical devices such as proton-conducting fuel cells (PCFC) and electrolyzers (PCEC) [1–8]. The design and production of such devices is part of the strategy of sustainable environmental development [9–16]. The most studied proton conductors are barium cerates-zirconates [17–24]. The barium zirconate crystallises in the classic perovskite ABO$_3$ structure. However, several years ago the possibility of proton transport was demonstrated for layered [25–26] and hexagonal perovskites [27–29]. Layered perovskites such as complex oxides materials based on nickelates lanthanides can be considered as efficient cathode materials [30–33]. Thus, the proton-conducting layered perovskites AA'BO$_4$ are very promising materials from the point of view of manufacturing PCFC/PCEC based on electrode and electrolyte with layered structure. The good

comparability between electrode and electrolyte materials with the same type of crystal structure can be expected.

Ionic conductivity for layered perovskites with the general formula AA'BO$_4$ were described for the compositions based on BaNdInO$_4$ [34–39], SrLaInO$_4$ [40–43], BaNdScO$_4$ [44], BaLaInO$_4$ [45], BaYInO$_4$ [38], BaGdInO$_4$ [38]. It was shown that method of heterovalent and isovalent doping can increase the ionic conductivity values by up to 1.5 orders of magnitude [25, 46, 47]. This paper first explores the possibility of heterovalent and isovalent doping of layered perovskites BaYInO$_4$ and BaGdInO$_4$.

2. Experimental

The compositions BaYInO$_4$, BaY$_{0.9}$La$_{0.1}$InO$_4$, BaY$_{0.9}$CaInO$_{3.95}$, BaY$_{0.9}$SrInO$_{3.95}$, BaY$_{0.9}$BaInO$_{3.95}$, BaYIn$_{0.9}$Ti$_{0.1}$O$_{4.05}$, BaGdInO$_4$, BaGd$_{0.9}$La$_{0.1}$InO$_4$, BaGd$_{0.9}$CaInO$_{3.95}$, BaGd$_{0.9}$SrInO$_{3.95}$, BaGd$_{0.9}$BaInO$_{3.95}$, BaGdIn$_{0.9}$Ti$_{0.1}$O$_{4.05}$ were prepared by the solid state method. The powders of the starting reagents

$BaCO_3$, $SrCO_3$, $CaCO_3$, La_2O_3, In_2O_3, Y_2O_3, Gd_2O_3, TiO_2 were dried and used in stoichiometric amounts. The agate mortar was used for grinding. The compositions were calcined after each grinding. The annealing was carried out in the temperature range of 800–1300 °C with 100 °C step.

The phase identification of the obtained compositions was carried out using the Bruker Advance D8 Cu Kα diffractometer.

The electrical conductivity was measured with an impedance spectrometer Z-1000P, Elins, RF. The investigations were carried out from 1000 to 200 °C with a cooling rate of 10/min under dry air or dry Ar. The dry gas (air or Ar) was prepared by circulating the gas through P_2O_5 ($pH_2O = 3.5 \cdot 10^{-5}$ atm). The wet gas (air or Ar) was obtained by bubbling the gas at room temperature first through distilled water and then through a saturated solution of KBr ($pH_2O = 2 \cdot 10^{-2}$ atm).

3. Results and Discussions

In this work, the isovalent doping of the lanthanum sublattice, $BaM_{0.9}La_{0.1}InO_4$ (M = Y, Gd), the heterovalent (acceptor) doping of this sublattice, $BaM_{0.9}M'InO_{3.95}$ (M = Y, Gd, M' = Ca, Sr, Ba), and the heterovalent (donor) doping of indium sublattice, $BaMIn_{0.9}Ti_{0.1}O_{4.05}$ (M = Y, Gd), were investigated. The XRD analysis showed that only matrix compositions, $BaYLaInO_4$ and $BaGdLaInO_4$, and the La-doped compositions, $BaY_{0.9}La_{0.1}InO_4$ and $BaGd_{0.9}La_{0.1}InO_4$, were obtained as single phases. Figure 1 represents the analysis of XRD data for these samples. The percentage of the target phase in the non-single-phase samples was 60–80, depending on the dopant.

The lattice parameters are provided in Table 1. The phases $BaYInO_4$ and $BaY_{0.9}La_{0.1}InO_4$ are indexed in the monoclinic symmetry (space group $P21/c$).
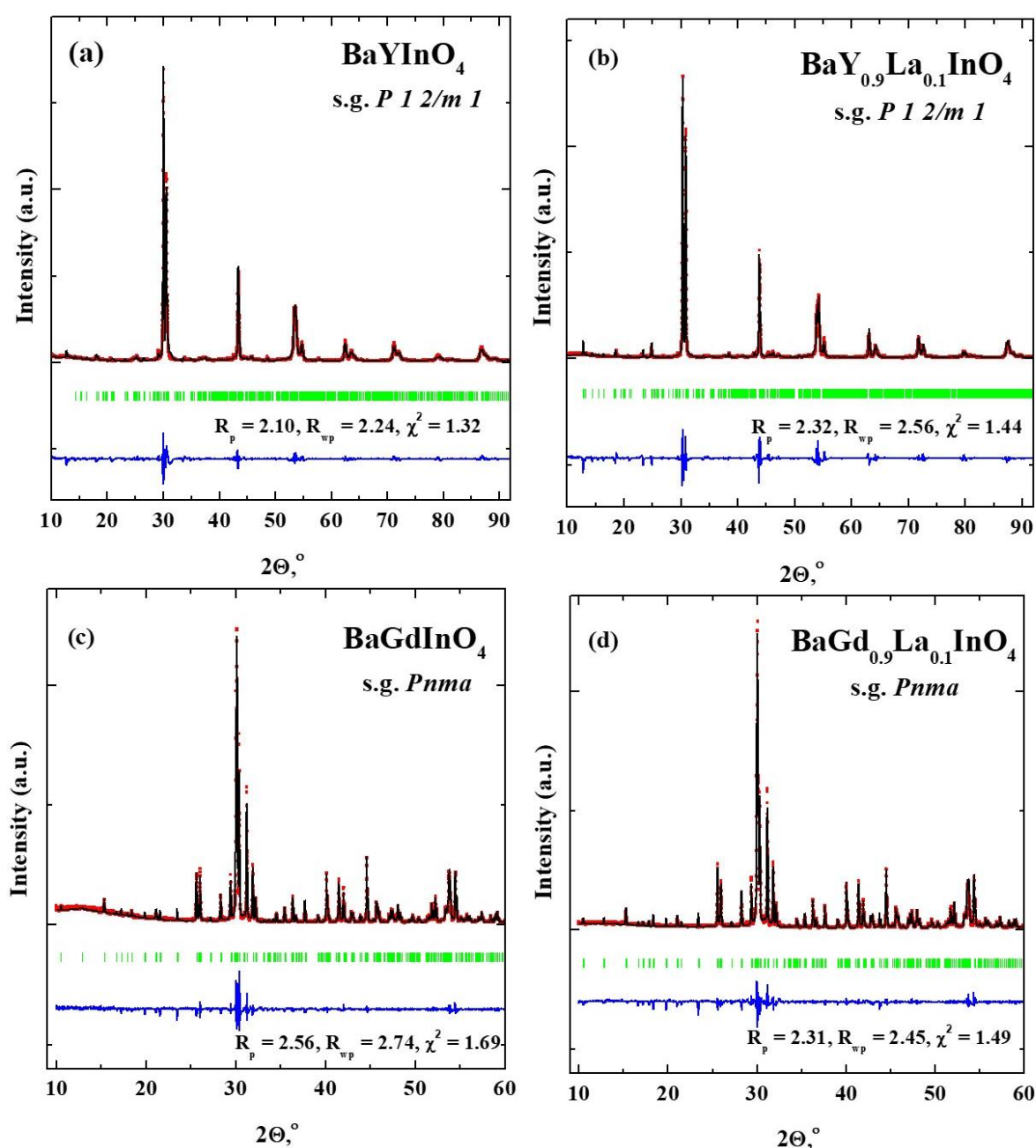
Figure 1 XRD patterns for the compositions $BaYInO_4$ (a), $BaY_{0.9}La_{0.1}InO_4$ (b), $BaGdInO_4$ (c) and $BaGd_{0.9}La_{0.1}InO_4$ (d).

The compositions $BaGdInO_4$ and $BaGd_{0.9}La_{0.1}InO_4$ are indexed in the orthorombic symmetry (space group *Pnma*). The obtained data for the undoped compositions are in the good agreement with the previous reported data [38]. As can be seen, the introduction of lanthanum ions with slightly bigger ionic radii ($r_{La^{3+}}$ = 1.216 Å, $r_{Gd^{3+}}$ = 1.107 Å, $r_{Y^{3+}}$ = 1.075 Å [48]) leads to the increase in the lattice parameters and unit cell volume. Figure 2 represents the XRD data for the doped compositions based on $BaGdLaInO_4$. The peaks belonging to unidentified impurities are marked. As we can see, the matrix phases $BaYLaInO_4$ and $BaGdLaInO_4$ have less tolerance to doping compared with $BaLaInO_4$, $SrLaInO_4$ and $BaNdInO_4$.

It is known that significant influence is exerted not only by the symmetry of the crystal and the ratio of the sizes of the cations, but also by the nature of the cations. We can suggest that the presence in the cation sublattice of combination of Ba/Y and Ba/Gd ions is not suitable for the formation of the oxygen defects (oxygen vacancy and oxygen interstitial) due to change in the energy of crystal compared with $BaLaInO_4$.

The typical EIS-plots are presented in Figure 3. The conductivity values were calculated from the resistance values taken at the point of intersection of the high-frequency semicircle with the x-axis.
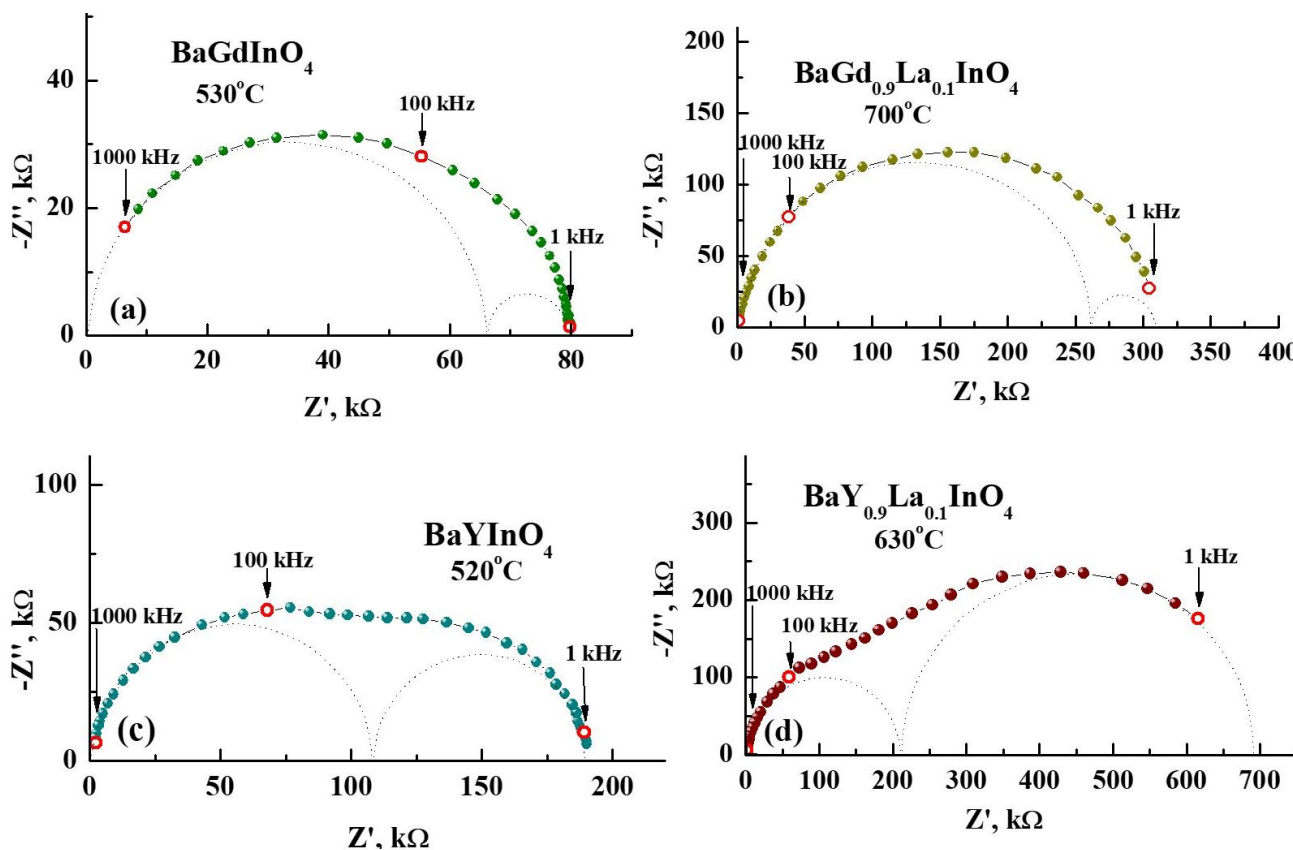
The temperature dependencies of the conductivity values for the compositions $BaGdInO_4$ and $BaGd_{0.9}La_{0.1}InO_4$ are presented in Figure 4a and Figure 4b, respectively.

**Table 1** Lattice parameters and unit cell volume for the investigated compositions.

Compostion	a, b (Å)	c (Å)	V_{cell} (Å³)
$BaGdInO_4$ [38]	13.7829	5.8835	10.6255
$BaGdInO_4$	13.7828	5.8833	10.6261
$BaGd_{0.9}La_{0.1}InO_4$	13.8075	5.8947	10.6434
$BaYInO_4$ [38]	8.96	5.95	8.32
$BaYInO_4$	8.9661	5.9514	8.3253
$BaY_{0.9}La_{0.1}InO_4$	9.0083	5.9494	8.3435
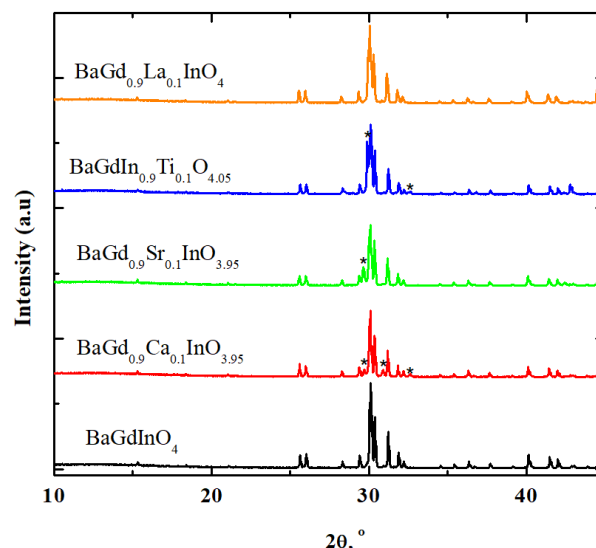
Figure 2 Comparison of XRD data for the compositions $BaGdInO_4$, $BaGd_{0.9}Ca_{0.1}InO_{3.95}$, $BaGd_{0.9}Sr_{0.1}InO_{3.95}$, $BaGdIn_{0.9}Ti_{0.1}O_{4.05}$ and $BaGd_{0.9}La_{0.1}InO_4$.


Figure 3 EIS plots for the compositions $BaGdInO_4$ (a), $BaGd_{0.9}La_{0.1}InO_4$ (b), $BaYInO_4$ (c) and $BaY_{0.9}La_{0.1}InO_4$ (d).
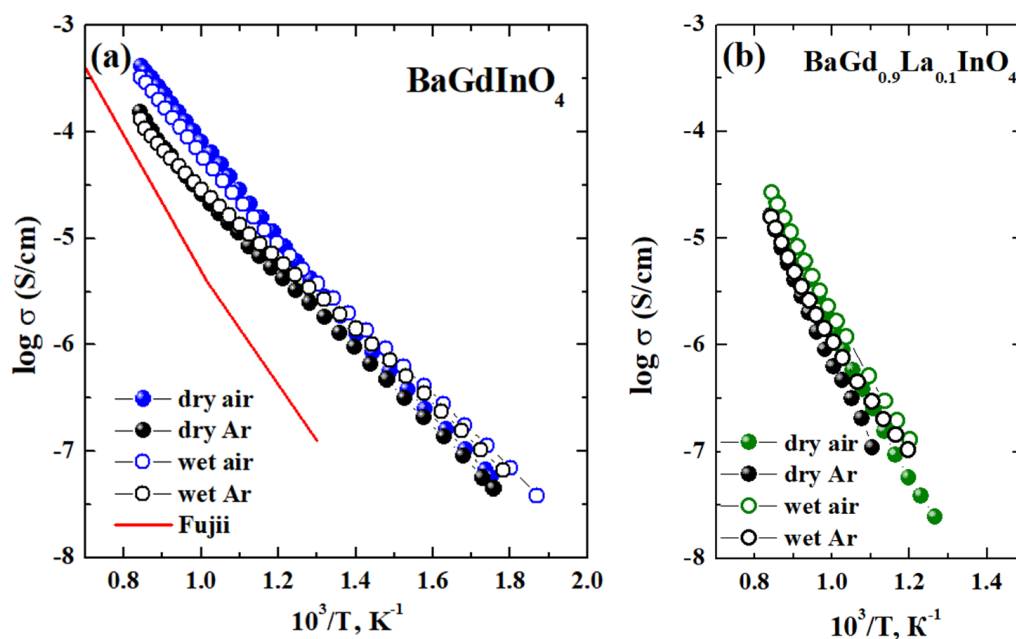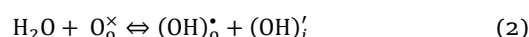
Figure 4 The temperature dependences of the conductivity for the compositions BaGdInO$_4$ (a) and BaGd$_{0.9}$La$_{0.1}$InO$_4$ (b) under dry (filled symbols) and wet (open symbols) conditions compared with data for BaGdInO$_4$ obtained by Fujii et al. (red line) [38].

The conductivity values for the undoped BaGdInO$_4$ compositions is higher that the data obtained by Fujii et al. [38]. Obviously, the reason for this is that the conductivity values in the work [38] were obtained in an atmosphere with uncontrolled humidity. The conductivity values under dry Ar ($pO_2 \sim 10^{-5}$ atm) are lower than those under dry air ($pO_2 = 0.21$ atm), indicating the hole contribution to the electrical conductivity:

$$\tfrac{1}{2}\,O_2 \Leftrightarrow O_i'' + 2h^\bullet \qquad (1)$$
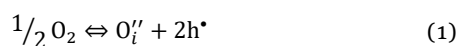
Thus, the nature of the electrical conductivity under dry air is the mixed ionic-hole. The conductivity values under wet atmosphere is higher than under dry atmosphere which indicates the appearance of a proton contribution to conductivity:

$$H_2O + O_O^\times \Leftrightarrow (OH)_O^\bullet + (OH)_i' \qquad (2)$$

The temperature dependences of the conductivity values for the doped BaGd$_{0.9}$La$_{0.1}$InO$_4$ composition are described by the same regularities (Figure 4b). However, the comparison of conductivity values for the compositions BaLaInO$_4$, BaGdInO$_4$ and BaGd$_{0.9}$La$_{0.1}$InO$_4$ (Figure 5) indicates that doping of BaGdInO$_4$ composition leads to the significant decrease in the conductivity values. At the same time, the Gd-containing composition BaGdInO$_4$ has higher conductivity values compared with La-containing composition BaLaInO$_4$ (about 0.5 order of magnitude).

Figure 6 represents the temperature dependences of the conductivity values for the compositions BaYInO$_4$ and BaY$_{0.9}$La$_{0.1}$InO$_4$. The discussion made earlier for the Gd-containing BaGdInO$_4$ and BaGd$_{0.9}$La$_{0.1}$InO$_4$ composition is also true for these the Y-containing compositions.

The conductivity values for all considered samples under dry air condition are presented in Figure 7. As we can see, among perovskites AA′BO$_4$ electrical conductivity values increase in the series BaYInO$_4$–BaLaInO$_4$–BaGdInO$_4$. In other words, Gd-containing composition is the most conductive among these matrix compositions. However, the doping is non-suitable strategy for the improving the electrical properties of this composition. The heterovalent (both acceptor and donor) doping does not allow obtaining single-phase compositions.

The isovalent doping leads to the decrease in the conductivity values. Further search for highly conductive materials with the layered perovskite structure can be aimed at materials with a different composition of the cation sublattice.
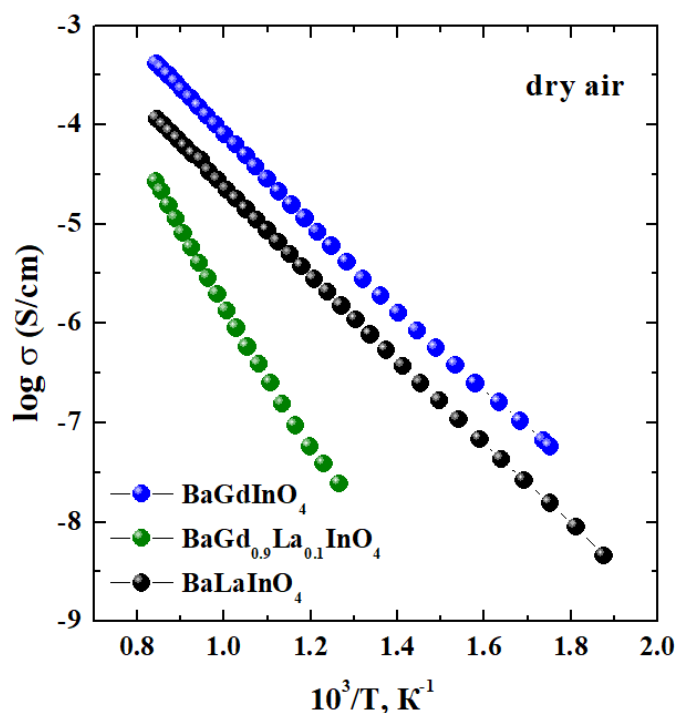
Figure 5 The temperature dependencies of the conductivity for the compositions BaLaInO$_4$, BaGdInO$_4$ and BaGd$_{0.9}$La$_{0.1}$InO$_4$ in dry air.
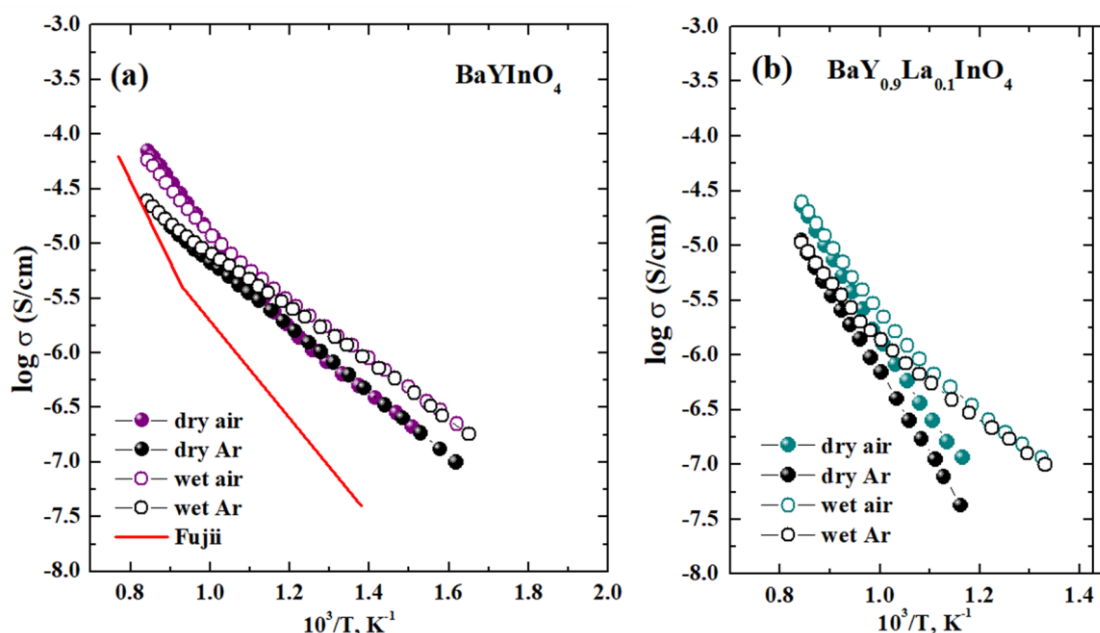
Figure 6 The temperature dependencies of the conductivity for the compositions $BaYInO_4$ (a) and $BaY_{0.9}La_{0.1}InO_4$ (b) under dry (filled symbols) and wet (open symbols) conditions compared with data for $BaYInO_4$ obtained by Fujii et al. (red line) [38].

4. Limitations

The main limitation is the difficulty in predicting the transport properties of complex oxides. The method of heterovalent and isovalent doping of cationic sublattices of layered perovskites was successfully applied for the compositions $BaNdInO_4$, $SrLaInO_4$, $BaLaInO_4$ with similar structure. However, for investigated matrix compositions this strategy was not successful.

5. Conclusions

In this paper, the possibility of heterovalent (acceptor and donor) and isovalent doping of La and In sublattices of layered perovskites $BaYLaInO_4$ and $BaGdLaInO_4$ was investigated for the first time. It was shown that both heterovalent (acceptor and donor) doping does not allow obtaining single-phase samples. The isovalent doping of Y(Gd) sublattice by La ions leads to the formation of single-phase compositions $BaY_{0.9}La_{0.1}InO_4$ and $BaGd_{0.9}La_{0.1}InO_4$. It was shown that doped compositions are characterized by lower conductivity values compared with undoped compositions. Among perovskites $AA'BO_4$ electrical conductivity increases in the series $BaYInO_4$ – $BaLaInO_4$ – $BaGdInO_4$. The nature of the electrical conductivity under dry air is the mixed ionic-hole conduction for all compositions. Further search for highly conductive materials with the layered perovskite structure can be aimed at materials with a different composition of the cation sublattice.

● Supplementary materials

No supplementary materials are available.

● Author contributions

Conceptualization: N.T., M.M.
Data curation: A.B., N.T.
Methodology: N.T., M.M.
Investigation: A.B., M.D., D.K., R.B.
Validation: A.G., N.T.
Visualization: A.G., N.T., M.M.
Writing – original draft: N.T.
Writing – review & editing: N.T.

● Conflict of interest

The authors declare no conflict of interest.

● Additional information

Author IDs:
    Natalia Tarasova, Scopus ID 37047923700;
    Maxim Mashkovtsev, Scopus ID 55012878800;
    Anzhelika Bedarkova, Scopus ID 58317277500.

Websites:

Institute of High Temperature Electrochemistry, https://ihte.ru/?page_id=3106;

Ural Federal University, https://urfu.ru/en/.

References

1. Zhang W, Hu YH. Progress in proton-conducting oxides as electrolytes for low-temperature solid oxide fuel cells: From materials to devices. Energy Sci Eng. 2021;9:984–1011. doi:10.1002/ese3.886

2. Nayak AP, Sasmal A. Recent advance on fundamental properties and synthesis of barium zirconate for proton conducting ceramic fuel cell. J Cleaner Prod. 2023;386:135827. doi:10.1016/j.jclepro.2022.135827

3. Guo R, He T. High-entropy perovskite electrolyte for protonic ceramic fuel cells operating below 600 ºC. ACS Mater Lett. 2022;4:1646–1652. doi:10.1021/acsmaterialslett.2c00542

4. Wang C, Li Z, Zhao S, Xia L, Zhu M, Han M, Ni M. Modelling of an integrated protonic ceramic electrolyzer cell (PCEC) for methanol synthesis. J Power Sources. 2023;559:232667. doi:10.1016/j.jpowsour.2023.232667

5. Liu F, Ding D, Duan C. Protonic ceramic electrochemical cells for synthesizing sustainable chemicals and fuels. Adv Sci. 2023;10:2206478. doi:10.1002/advs.202206478

6. Kim D, Bae KT, Kim KJ, Im H-N, Jang S, Oh S, Lee SW, Shin TH, Lee KT. High-performance protonic ceramic electrochemical cells. ACS Energy Lett. 2022;7:2393–2400. doi:10.1021/acsenergylett.2c01370

7. Tian H, Luo Z, Song Y, Zhou Y, Gong M, Li W, Shao Z, Liu M, Liu X. Protonic ceramic materials for clean and sustainable energy: Advantages and challenges. Int Mater Rev. 2022;0:1–29. doi:10.1080/09506608.2022.2068399

8. Ji HI, Lee JH, Son JW, Yoon KJ, Yang S, Kim BK. Protonic ceramic electrolysis cells for fuel production: A brief review. J Korean Ceram Soc. 2020;57:480–494. doi:10.1007/s43207-020-00059-4

9. Corigliano O, Pagnotta L, Fragiacomo P. On the technology of solid oxide fuel cell (SOFC) energy systems for stationary power generation: A review. Sustainability. 2022;14:15276. doi:10.3390/su142215276

10. Kumar SS, Lim H. An overview of water electrolysis technologies for green hydrogen production. Energy Rep. 2022;8:13793–13813. doi:10.1016/j.egyr.2022.10.127

11. Huang L, Huang X, Yan J, Liu Y, Jiang H, Zhang H, Tang J, Liu Q. Research progresses on the application of perovskite in adsorption and photocatalytic removal of water pollutants. J Hazard Mater. 2023;442:130024. doi:10.1016/j.jhazmat.2022.130024

12. Tarasova N. Layered perovskites $BaLn_nIn_nO_{3n+1}$ (n = 1, 2) for electrochemical applications: A mini review. Membranes. 2023;13:34. doi:10.3390/membranes13010034

13. Zvonareva IA, Medvedev DA. Proton-conducting barium stannate for high-temperature purposes: A brief review. J Eur Ceram Soc. 2023;43:198–207. doi:10.1016/j.jeurceramsoc.2022.10.049

14. Aminudin MA, Kamarudin SK, Lim BH, Majilan EH, Masdar MS, Shaari N. An overview: Current progress on hydrogen fuel cell vehicles. Int J Hydrogen Energy. 2023;48:4371–4388. doi:10.1016/j.ijhydene.2022.10.156

15. Liu F, Fang L, Diercks D, Kazempoor P, Duan C. Rationally designed negative electrode for selective CO_2-to-CO conversion in protonic ceramic electrochemical cells. Nano Energy 2022;102:107722. doi:10.1016/j.nanoen.2022.107722

16. Liu F, Duan C. Direct-hydrocarbon proton-conducting solid oxide fuel cells. Sustainability. 2021;13:4736. doi:10.3390/su13094736

17. Nayak AK, Sasmal A. Recent advance on fundamental properties and synthesis of barium zirconate for proton conducting ceramic fuel cell. J Clean Prod. 2023;386:135827. doi:10.1016/j.jclepro.2022.135827

18. Qiao Z, Li S, Li Y, Xu N, Xiang K. Structure, mechanical properties, and thermal conductivity of $BaZrO_3$ doped at the A-B site. Ceram Int. 2022;48;12529–12536. doi:10.1016/j.ceramint.2022.01.120

19. Guo R, Li D, Guan R, Kong D, Cui Z, Zhou Z, He T. Sn–Dy–Cu triply doped $BaZr_{0.1}Ce_{0.7}Y_{0.2}O_{3-\delta}$: A chemically stable and highly proton-conductive electrolyte for low-temperature solid oxide fuel cells. ACS Sustain Chem Eng. 2022;10:5352–5362. doi:10.1021/acssuschemeng.2c00807

20. Gu Y, Luo G, Chen Z, Huo Y, Wu F. Enhanced chemical stability and electrochemical performance of $BaCe_{0.8}Y_{0.04}Ni_{0.04}Sm_{0.06}O_{3-\delta}$ perovskite electrolytes as proton conductors. Ceram Int. 2022;48:10650–10658. doi:10.1016/j.ceramint.2021.12.279

21. Medvedev DA. Current drawbacks of proton-conducting ceramic materials: How to overcome them for real electrochemical purposes. Curr Opin Green Sustain Chem. 2021;32:100549. doi:10.1016/j.cogsc.2021.100549

22. Kasyanova AV, Zvonareva IA, Tarasova NA, Bi L, Medvedev DA, Shao Z. Electrolyte materials for protonic ceramic electrochemical cells: Main limitations and potential solutions. Mater Rep Energy. 2022;2:100158. doi:10.1016/j.matre.2022.100158

23. Tarutina L, Starostina I, Vdovin G., Pershina S, Vovkotrub A, Murashkina A. Chemical stability aspects of $BaCe_{0.7-x}Fe_xZr_{0.2}Y_{0.1}O_{3-\delta}$ mixed ionic-electronic conductors as promising electrodes for protonic ceramic fuel cells. Chim Tehno Acta. 2023;10(4):202310414. doi:10.15826/chimtech.2023.10.4.14

24. Danilov NA, Starostina IA, Starostin GN, Kasyanova AV, Medvedev DA. Fundamental Understanding and Applications of Protonic Y-and Yb-Coped $Ba(Ce,Zr)O_3$ perovskites: state-of-the-art and perspectives. Adv Energy Mater. 2023;13(47):2302175. doi:10.1002/aenm.202302175

25. Tarasova N, Animitsa I. Materials $A^{II}LnInO_4$ with Ruddlesden-Popper structure for electrochemical applications: Relationship between ion (oxygen-ion, proton) conductivity, water uptake and structural changes. Mater. 2022;15:114. doi:10.3390/ma15010114

26. Tarasova N. Layered perovskites $BaLn_nIn_nO_{3n+1}$ (n = 1, 2) for electrochemical applications: a mini review. Membranes. 2023;13:34. doi:10.3390/membranes13010034

27. Andreev RD, Korona DV, Anokhina IA, Animitsa IE. Novel Nb^{5+}-doped hexagonal perovskite $Ba_5In_2Al_2ZrO_{13}$ (structure, hydration, electrical conductivity). Chimica Tehno Acta. 2022;9(4):20229414. doi:10.15826/chimtech.2022.9.4.14

28. Andreev RD, Anokhina IA, Korona DV, Gilev AR, Animitsa IE. Transport properties of In^{3+}- and Y^{3+}-doped hexagonal perovskite $Ba_5In_2Al_2ZrO_{13}$. Russ J Electrochem. 2023;59(3):190–203. doi:10.1134/S1023193523030035

29. Andreev RD, Animitsa IE. Protonic transport in the novel complex oxide $Ba_5Y_{0.5}In_{1.5}Al_2ZrO_{13}$ with intergrowth structure. Ionics. 2023;29(11):4647–4658. doi:10.1007/s11581-023-05187-5

30. Tarutin A, Lyagaeva J, Medvedev D, Bi L, Yaremchenko A. Recent advances in layered $Ln_2NiO_{4+\delta}$ nickelates: fundamentals and prospects of their applications in protonic ceramic fuel and electrolysis cells. J Mater Chem A. 2021;9(1):154–195. doi:10.1039/D0TA08132A

31. Tarutin A, Gorshkov Yu, Bainov A, Vdovin G, Vylkov A, Lyagaeva J, Medvedev D. Barium-doped nickelates $Nd_{2-x}Ba_xNiO_{4+\delta}$ as promising electrode materials for protonic ceramic electrochemical cells. Ceram Int. 2020;46(15):24355–24364. doi:10.1016/j.ceramint.2020.06.217

32. Tarutin A, Lyagaeva J, Farlenkov A, Plaksin S, Vdovin G, Demin A, Medvedev D. A reversible protonic ceramic cell with symmetrically designed $Pr_2NiO_{4+\delta}$-based electrodes: fabrication and electrochemical features. Mater. 2019;12(1):118. doi:10.3390/ma12010118

33. Tarutin AP, Lyagaeva JG, Farlenkov AS, Vylkov AI, Medvedev DA. Cu-substituted $La_2NiO_{4+\delta}$ as oxygen electrodes for

protonic ceramic electrochemical cells. Ceram Int. 2019;45(13):16105–16112. doi:10.1016/j.ceramint.2019.05.127

34. Fujii K, Esaki Y, Omoto K, Yashima M, Hoshikawa A, Ishigaki T, Hester JR. New perovskite-related structure family of oxide-ion conducting materials NdBaInO$_4$. Chem Mater. 2014;26:2488–2491. doi:10.1021/cm500776x

35. Fujii, K, Shiraiwa, M, Esaki, Y, Yashima, M, Kim, S.J, Lee. S. Improved oxide-ion conductivity of NdBaInO$_4$ by Sr doping. J Mater Chem A 2015;3:11985. doi:10.1039/c5ta01336d

36. Ishihara T, Yan Yu, Sakai T, Ida S. Oxide ion conductivity in doped NdBaInO$_4$. Solid State Ion. 2016;288:262. doi:10.1016/j.ssi.2016.01.011

37. Yang X, Liu S, Lu F, Xu J, Kuan, X. Acceptor doping and oxygen vacancy migration in layered perovskite NdBaInO$_4$-based mixed conductors. J Phys Chem C. 2016;120:6416–6426. doi:10.1021/acs.jpcc.6b00700

38. Fijii K, Yashima M. Discovery and development of BaNdInO$_4$ – A brief review. J Ceram Soc Jpn. 2018;126:852–859. doi:10.2109/jcersj2.18110

39. Zhou Y, Shiraiwa M, Nagao M, Fujii K, Tanaka I, Yashima M, Baque L, Basbus JF, Mogni LV, Skinner SJ. Protonic conduction in the BaNdInO$_4$ structure achieved by acceptor doping. Chem Mater. 2021;33:2139–2146. doi:10.1021/acs.chemmater.0c04828

40. Troncoso L, Alonso JA, Aguadero A. Low activation energies for interstitial oxygen conduction in the layered perovskites La$_{1+x}$Sr$_{1-x}$InO$_{4+d}$. J Mater Chem A. 2015;3:17797–17803. doi:10.1039/c5ta03185k

41. Troncoso L, Alonso JA, Fernández-Díaz MT, Aguadero A. Introduction of interstitial oxygen atoms in the layered perovskite LaSrIn$_{1-x}$B$_x$O$_{4+\delta}$ system (B=Zr, Ti). Solid State Ion. 2015;282:82–87. doi:10.1016/j.ssi.2015.09.014

42. Troncoso L, Mariño C, Arce MD, Alonso JA. Dual oxygen defects in layered La$_{1.2}$Sr$_{0.8-x}$Ba$_x$InO$_{4+d}$ (x = 0.2, 0.3) oxide-ion conductors: A neutron diffraction study. Mater. 2019;12:1624. doi:10.3390/ma12101624

43. Troncoso L, Arce MD, Fernández-Díaz MT, Mogni LV, Alonso JA. Water insertion and combined interstitial-vacancy oxygen conduction in the layered perovskites La$_{1.2}$Sr$_{0.8-x}$Ba$_x$InO$_{4+\delta}$. New J Chem. 2019;43:6087–6094. doi:10.1039/C8NJ05320K

44. Shiraiwa M, Kido T, Fujii K, Yashima M. High-temperature proton conductors based on the (110) layered perovskite BaNdScO$_4$. J Mat Chem A. 2021;9:8607. doi:10.1039/D0TA11573H

45. Tarasova N, Animitsa I, Galisheva A, Korona D. Incorporation and conduction of protons in Ca, Sr, Ba-doped BaLaInO$_4$ with Ruddlesden-Popper structure. Mater. 2019;12:1668. doi:10.3390/ma12101668

46. Tarasova N, Galisheva A, Animitsa I. Ba^{2+}/Ti^{4+}- co-doped layered perovskite BaLaInO$_4$: the structure and ionic (O^{2-}, H$^+$) conductivity. Int J Hydrog Energy. 2021;46(32):16868–16877. doi:10.1016/j.ijhydene.2021.02.044

47. Tarasova N, Galisheva A, Animitsa I, Anokhina I, Gilev A, Cheremisina P. Novel mid-temperature Y^{3+} → In^{3+} doped proton conductors based on the layered perovskite BaLaInO$_4$. Ceram Int. 2022;48:15677–15685. doi:10.1016/j.ceramint.2022.02.102

48. Shannon RD. Revised effective ionic radii and systematic studies of interatomic distances in halides and chalcogenides. Acta Cryst. 1976;A32:751–767. doi:10.1107/S0567739476001551